

Communication

# UV-Induced Gold Nanoparticle Growth in Polystyrene Matrix with Soluble Precursor

Andrey Kudryashov <sup>1</sup>, Svetlana Baryshnikova <sup>1,2</sup>, Sergey Gusev <sup>3</sup>, Dmitry Tatarskiy <sup>3,4</sup>, Ivan Lukichev <sup>1</sup>, Nadezhda Agareva <sup>1</sup>, Andrey Poddel'sky <sup>2</sup> and Nikita Bityurin <sup>1,\*</sup>

<sup>1</sup> Institute of Applied Physics of the Russian Academy of Sciences, 46 Ul'yanov Street, 603950 Nizhny Novgorod, Russia

<sup>2</sup> G.A. Razuvaev Institute of Organometallic Chemistry of the Russian Academy of Sciences, 49 Tropinina Str., 603950 Nizhny Novgorod, Russia

<sup>3</sup> Institute of Physics of Microstructures of the Russian Academy of Sciences, GSP-105, 603950 Nizhny Novgorod, Russia

<sup>4</sup> Faculty of Physics, N.I. Lobachevsky State University of Nizhny Novgorod, 23 Gagarin Ave, 603950 Nizhny Novgorod, Russia

\* Correspondence: bit@appl.sci-nnov.ru

**Abstract:** It is demonstrated that UV (LED at 365 nm) irradiation with subsequent heating (90–110 °C) of the polystyrene matrix containing a soluble Au(I) compound ((Ph<sub>3</sub>P)Au(*n*-Bu)) results in the growth of gold nanoparticles within the sample bulk, as confirmed by UV-vis spectroscopy and TEM electron microscopy. Pure heating of the samples without previous UV irradiation does not provide gold nanoparticles, thereby facilitating optical image printing. Comparing the nanoparticles' growth kinetics in samples with different precursor content suggests the nanoparticle growth mechanism through Au(I) autocatalytic reduction at the surface of a gold nanoparticle. Within the polymer matrix, this mechanism is suggested for the first time.

**Keywords:** gold nanoparticles; photoinduced nanocomposites; polystyrene matrix; Au(I) precursor; auto-catalytic growth; plasmonic structures



**Citation:** Kudryashov, A.; Baryshnikova, S.; Gusev, S.; Tatarskiy, D.; Lukichev, I.; Agareva, N.; Poddel'sky, A.; Bityurin, N. UV-Induced Gold Nanoparticle Growth in Polystyrene Matrix with Soluble Precursor. *Photonics* **2022**, *9*, 776. <https://doi.org/10.3390/photonics9100776>

Received: 23 September 2022

Accepted: 16 October 2022

Published: 19 October 2022

**Publisher's Note:** MDPI stays neutral with regard to jurisdictional claims in published maps and institutional affiliations.



**Copyright:** © 2022 by the authors. Licensee MDPI, Basel, Switzerland. This article is an open access article distributed under the terms and conditions of the Creative Commons Attribution (CC BY) license (<https://creativecommons.org/licenses/by/4.0/>).

## 1. Introduction

Among the diversity of organic–inorganic nanomaterials suitable for photonics [1–3], nanocomposite materials consisting of inorganic nanoparticles embedded in a polymer matrix are objects of growing interest of modern nanotechnology owing to their unique optical, mechanical, and chemical properties [4]. A vital role here belongs to photoinduced nanocomposites, in which nanoparticles appear just after irradiation of an initially homogeneous matrix containing a precursor [5]. The formation of nanoparticles significantly changes the optical properties of the matrix, permitting one to generate patterns composed of either plasmonic (metallic) or excitonic (semiconductor) nanoparticles by means of laser writing [6] or mask-mediated techniques [7]. Such approaches allow one to use these materials for photonics applications [6,8], in particular, as gradient-index media [9].

Different matrices are employed for the nanocomposites. Among them, polystyrene is promising, owing to its optical transparency, good thermo-mechanic properties, and ease of sample preparation. There is an important aspect associated with photoinduced nanocomposites with several precursors within the same matrix [8]. The successful solution of this problem could result in obtaining photoinduced two- or several-component structures, e.g., core-shell nanoparticles [10], and more elaborated objects. The diversity of the matrices is a very helpful tool for choosing different sets of precursors to elaborate sophisticated photonics structures on the basis of photoinduced nanocomposites. The photoinduced polystyrene-based nanocomposites with semiconductor nanoparticles have been reported [11]. There is, however, a problem with gold-containing photoinduced nanocomposites with the polystyrene matrix.

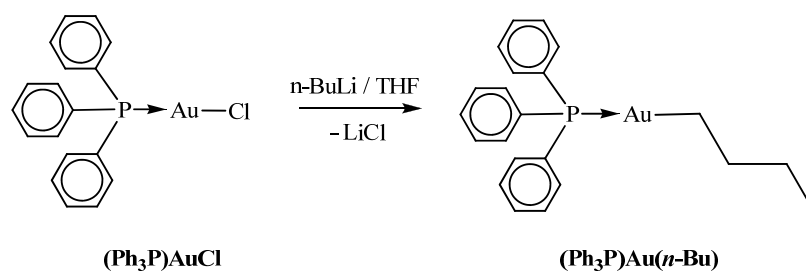
Several publications dealing with the investigation of the gold nanoparticle growth process in solutions (mainly in water or water-alcohol mixture) or suspension use the photochemical or chemical reduction of gold(III) compounds as starting reagents [12–15]. However, such gold(III) precursors of gold nanoparticles are not soluble in most organic solvents, which seriously complicates their use in the preparation of polystyrene-based nanocomposites. Thus, the most popular gold precursor  $\text{HAuCl}_4$  useful for photoinduced nanocomposites based on the PMMA matrix [16] is incompatible with polystyrene.

Numerous publications have reported the precursor-based gold nanoparticles containing polystyrene nanocomposites [17–23]. These papers deal with the gold(I) thiolate—polystyrene blends. The reported precursors have two features in common: they are poorly soluble, and both the gold nanoparticles initiation and the growth processes are purely thermally activated.

In the present publication, we report the photoinduced polystyrene-based nanocomposite with an alternative precursor. We use a toluene soluble gold(I)-containing compound  $(\text{Ph}_3\text{P})\text{Au}(n\text{-Bu})$ , assuming its good solubility in polystyrene and possible compatibility with toluene soluble precursors of semiconductor nanoparticles studied earlier [12,13]. We show that initial non-irradiated samples (polystyrene + precursor) remain intact when heated at moderate temperatures. However, after being UV-irradiated and heated, the same samples demonstrate the growth of gold nanoparticles. This significantly differs from the results obtained earlier [17–23]. We follow the kinetics of this process by studying the evolution of the optical spectra. We used this approach in our previous publications elucidating the CdS and gold nanoparticle growth in PMMA matrix [13,16]. The gold(I)-containing compound has been reported as a gold precursor in PMMA in ref. [8]. In the present publication, unlike our previous studies, we compare the results for samples with different precursor content. This allows us to suggest a new mechanism of the nanoparticles' growth in polymer films.

## 2. Materials and Methods

The triphenylphosphine gold(I) complex with *n*-butyl group  $(\text{Ph}_3\text{P})\text{Au}(n\text{-Bu})$  was prepared by the reaction of the presynthesized triphenylphosphine gold(I) chloride  $(\text{Ph}_3\text{P})\text{AuCl}$  with *n*-butyl lithium in an equimolar ratio in a tetrahydrofuran (THF) medium (Scheme 1).



**Scheme 1.** Synthesis of the alkylgold derivative  $(\text{Ph}_3\text{P})\text{Au}(n\text{-Bu})$ .

The gold(I) derivatives  $(\text{Ph}_3\text{P})\text{Au}(\text{Alkyl})$  were synthesized using a modification of the method described in ref. [14] for the synthesis of  $(\text{Ph}_3\text{P})\text{Au}(\text{SC}_{12}\text{H}_{25})$ . At the first stage, the precursor  $(\text{Ph}_3\text{P})\text{AuCl}$  was prepared by the reaction of  $\text{HAuCl}_4$  with  $\text{Ph}_3\text{P}$  in a methanol solution in the molar ratio 1:2 (the reagents were rigorously mixed in methanol at ambient temperature until a complete color change from saturated bright yellow to almost colorless pale yellow and complete precipitation of a white powder  $(\text{Ph}_3\text{P})\text{AuCl}$  occurred). The second stage—the reaction of  $(\text{Ph}_3\text{P})\text{AuCl}$  with *n*-butyl lithium—was performed in the THF solution under reduced pressure in the absence of oxygen and air moisture by stirring at  $-40^\circ\text{C}$  for 20 min. Then, the temperature was slowly increased to an ambient level ( $\sim 22^\circ\text{C}$ ) and the stirring was continued for 1 day. The evaporation of the solvent under reduced pressure resulted in a product  $(\text{Ph}_3\text{P})\text{Au}(n\text{-Bu})$  as a transparent oil stable on air at room temperature during a few days and soluble in common organic solvents such as *n*-pentane, toluene, or THF. The gold(I) complex  $(\text{Ph}_3\text{P})\text{Au}(n\text{-Bu})$  was studied by  $^1\text{H}$  and  $^{13}\text{C}$  NMR spectroscopy (the NMR spectra were registered using Bruker AVANCE

New (300 MHz) spectrometer with TMS as internal reference and  $\text{CDCl}_3$  as solvent), IR—spectroscopy (IR spectra were monitored in the  $400\text{--}4000\text{ cm}^{-1}$  range by a FSM 1201 Fourier-IR spectrometer in Nujol mulls), and elemental analysis. The spectroscopic data of this complex correspond to those reported earlier in [15], e.g., according to the  $^1\text{H}$  NMR spectroscopy ( $\text{CDCl}_3$ , 300 MHz) the methyl group protons give rise to a triplet with  $^3J(\text{H,H}) = 7.3\text{ Hz}$  at 0.98 ppm, the methylene groups signals appear as two multiplets at the ranges 1.4–1.6 and 1.8–2.0 ppm, and the aromatic region contains multiplet at 7.4–7.6 ppm of phenyl protons of the  $\text{Ph}_3\text{P}$  ligand.

Polystyrene films with a thickness of about  $200\text{ }\mu\text{m}$  with the  $(\text{Ph}_3\text{P})\text{Au}(n\text{-Bu})$  gold precursor embedded in them were obtained by pouring from a solution of the polymer with the precursor in toluene. The films are transparent in the visible range; the initial spectrum is shown in Figure 1.

An NVSU233A UV LED (Nichia, Japan) with a central wavelength of 365 nm was chosen as the radiation source; the emission spectrum is shown in Figure 1. The absorbance was measured using a spectrophotometer (Shimadzu UV1800). Heating of the samples was performed in an oven.

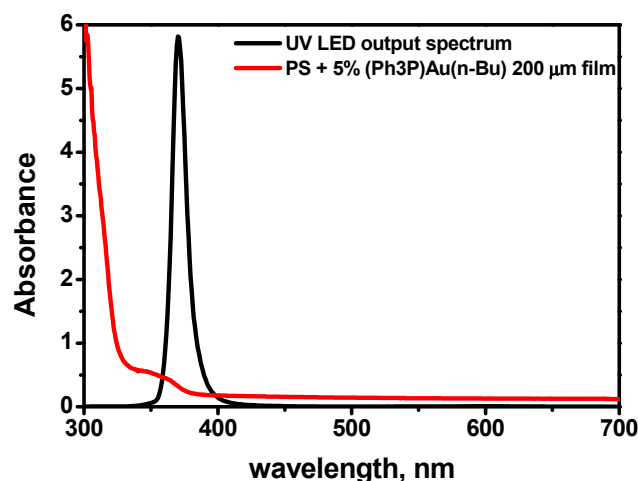


**Figure 1.** The optical spectrum of the initial just-obtained polystyrene films with  $(\text{Ph}_3\text{P})\text{Au}(n\text{-Bu})$  precursor (5 wt %) (red) and UV LED emission spectrum (arbitrary units) (black).

The work was carried out with two types of samples: polystyrene films containing 5 wt % and 2.5 wt % of  $(\text{Ph}_3\text{P})\text{Au}(n\text{-Bu})$ .

The crystalline structure of the nanoparticles was investigated by means of transmission electron microscopy methods. High-resolution transmission electron microscopy (HRTEM) images were acquired with a LIBRA 200 MC Schottky Field emission gun microscope (Carl Zeiss SMT, Oberkochen Germany) operating at 200 kV. For TEM sample preparation, a drop of treated film solution in toluene was deposited on a thin (30 nm)  $\text{Si}_3\text{N}_4$  membrane with spin-coating at  $\sim 2000\text{ rpm}$ . After that, the polymer films were processed in soft oxygen plasma using Evactron 25/45 De-Contaminating RF Plasma Cleaning System (XEI Scientific, Inc., Redwood City, CA, USA). This processing was used to remove the organic matrix of the samples. The TEM images were acquired and processed with Digital Micrograph software (Gatan, Inc., Pleasanton, CA, USA).

### 3. Results and Discussion

Figures 2 and 3 show that a broad extinction band in the visible range appears just after irradiation of the samples at room temperature. After heating at temperatures of  $95\text{--}110\text{ }^\circ\text{C}$ , the visual absorption increases, forming a band with the maximum at the wavelengths close to 540 nm, which is characteristic of the plasmon resonance in gold nanoparticles in polystyrene. Experimentally, it was found that the film is colored uniformly under exposure

exceeding 30 min irradiation at the intensity  $I = 90 \text{ mW/cm}^2$ . The TEM images confirm the existence of gold nanoparticles in the treated samples.

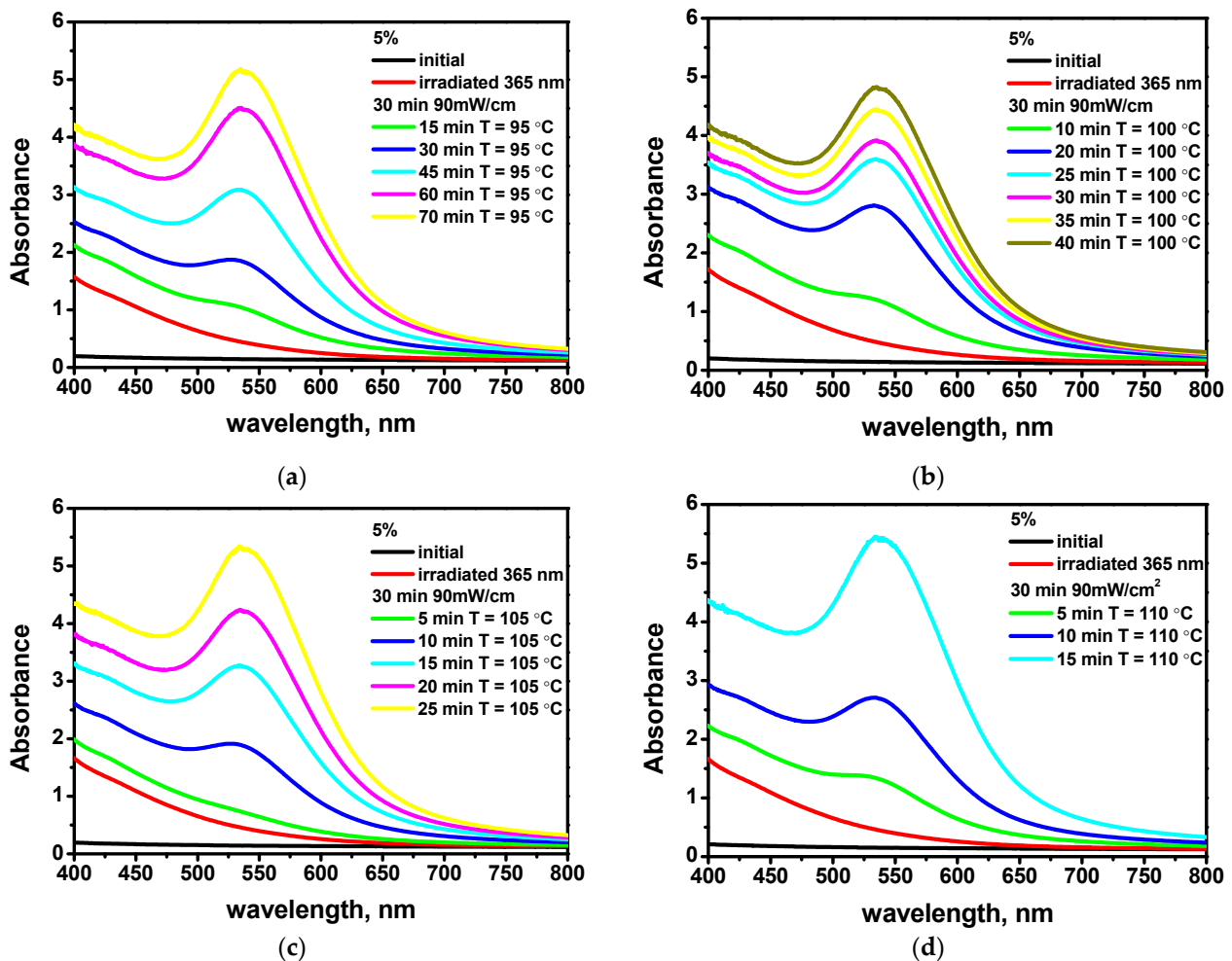


**Figure 2.** Absorbance of samples of polystyrene + 5 wt %  $(\text{Ph}_3\text{P})\text{Au}(n\text{-Bu})$ : initial, after irradiation and after further heating at temperatures of (a)  $95^\circ\text{C}$ , (b)  $100^\circ\text{C}$ , (c)  $105^\circ\text{C}$ , and (d)  $110^\circ\text{C}$ .

An HRTEM micrograph of the LED-irradiated sample is presented in Figure 4a, showing an accumulation of nanoparticles with sizes of about 10–20 nm. All particles have a well-defined crystal structure. The inset in the upper right corner of the Figure 4a is an enlarged fragment of the image of one of the selected particles, which clearly shows the crystal lattice with the parameter of 0.204 nm. This parameter corresponds to the distance between crystal planes (200) of metallic gold.

The selected area electron diffraction (SAED) of this cluster of nanoparticles (Figure 4b) also corresponds to lattice constants  $d_1 = 0.235 \pm 0.003 \text{ nm}$ ,  $d_2 = 0.204 \pm 0.002 \text{ nm}$ ,  $d_3 = 0.144 \pm 0.002 \text{ nm}$ , and  $d_4 = 0.123 \pm 0.002 \text{ nm}$ , which can be indicated as reflections of the planes with indices (111), (200), (220), and (113), respectively, for metallic Au lattice (see red circles in Figure 4b).

Heating of these samples at a temperature lower than  $110^\circ\text{C}$  without the previous irradiation does not provide any nanoparticles. This is confirmed by the image shown in Figure 5. Here, the irradiated regions demonstrate red color after heating, whereas the non-irradiated parts of the same samples remain intact.

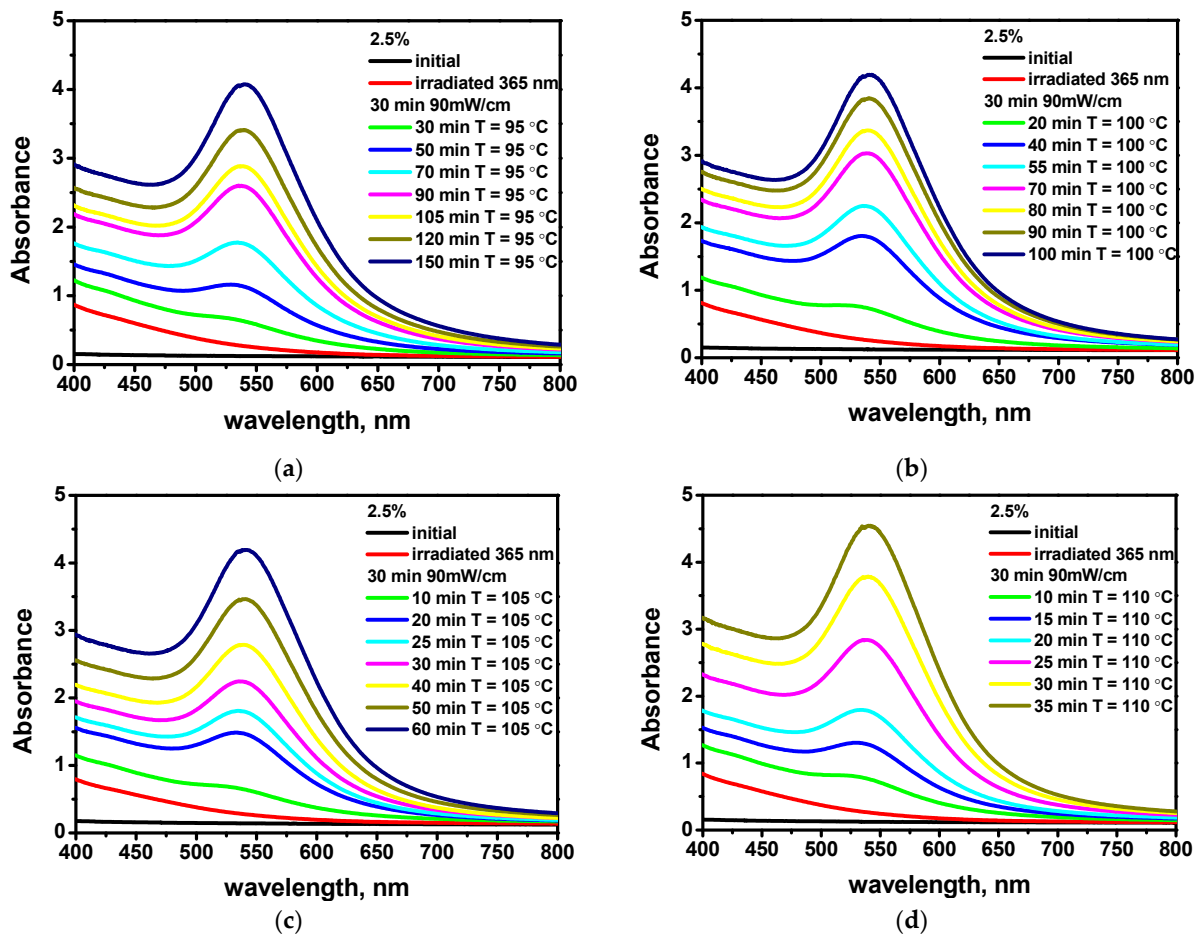


Figure 3. Absorbance of samples of polystyrene + 2.5 wt % (Ph<sub>3</sub>P)Au(*n*-Bu): initial, after irradiation and after further heating at temperatures of (a) 95 °C, (b) 100 °C, (c) 105 °C, and (d) 110 °C.

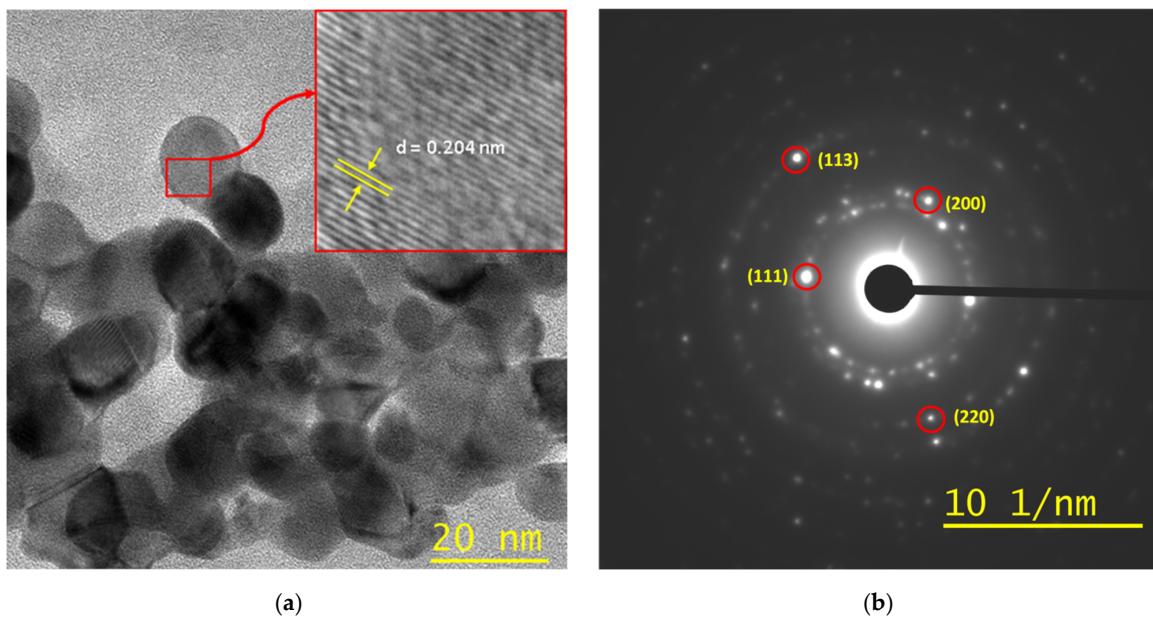
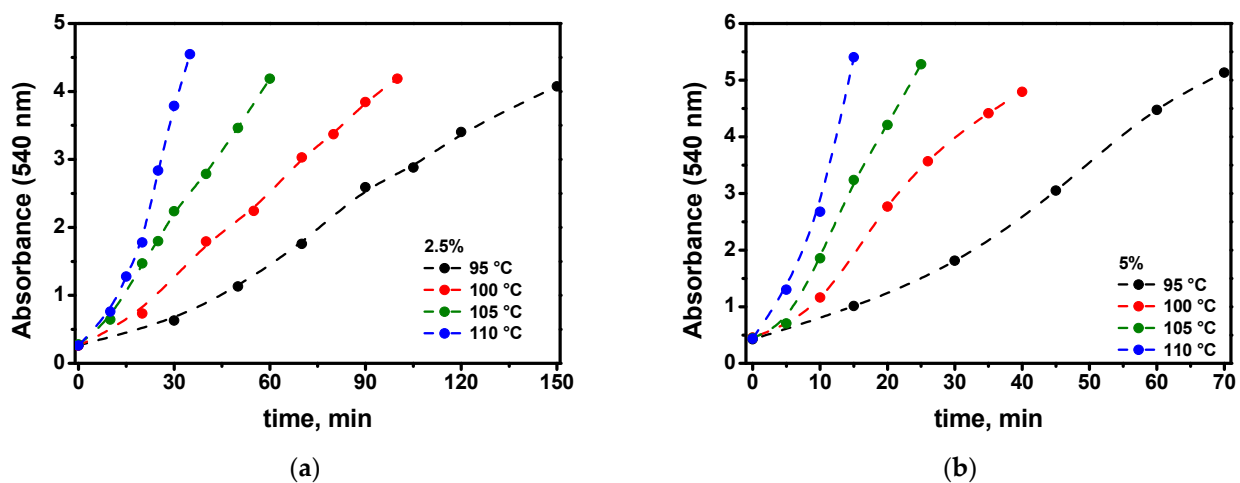


Figure 4. (a) HRTEM micrographs of nanoparticles formed in the irradiated film. (b) The SAED patterns for the cluster of nanoparticles on (a). Red circles show reflections of the corresponding planes of metallic Au lattice.



**Figure 5.** The sample after irradiation through the mask and further heating.

The kinetics of the absorbance of samples at a wavelength of 540 nm under the effect of heating are presented in Figure 6. The initial moment of time corresponds to the sample after UV irradiation. At lower temperatures (95 °C), the rate of increase in absorbance slows down, and the graphs show saturation. At a temperature of 110 °C, the saturation is not observed. It probably occurs at further heating, but in this case the absorbance becomes too strong, and the corresponding measurements are restricted by the noise in spectrophotometer.



**Figure 6.** Absorbance of samples polystyrene + (Ph<sub>3</sub>P)Au(*n*-Bu) 2.5% (a) and 5% (b) at a wavelength of 540 nm depending on the heating time at four different temperatures.

We have tested the dependence of the nanoparticle formation process on the irradiation intensity. The experiment was performed with irradiation at a lower intensity but with the same exposure (50 min 54 mW/cm<sup>2</sup> instead of 30 min 90 mW/cm<sup>2</sup>) (Figure 7).

After irradiation with a lower intensity at the same exposure, the same absorption occurs. Upon further heating, as seen in Figure 7, the results also agree well for both the 5% and 2.5% films. This means that the UV-induced absorption is determined by the exposure, that is, by the product of the light intensity and the irradiation time.

An experiment was also carried out in which a 5% film was irradiated for 30 min, and a 2.5% film was irradiated for 80 min, with an intensity of 90 mW/cm<sup>2</sup> so that the absorption of these films after irradiation was the same. Then, the growth of the plasmon peak upon heating was studied (Figure 8).

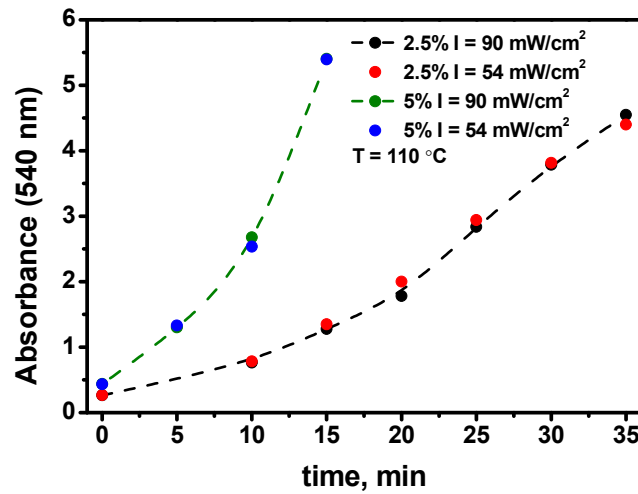


Figure 7. Comparison of the dependence of the absorbance of samples on the heating time at 110 °C after irradiation at different intensities and with the same exposure.

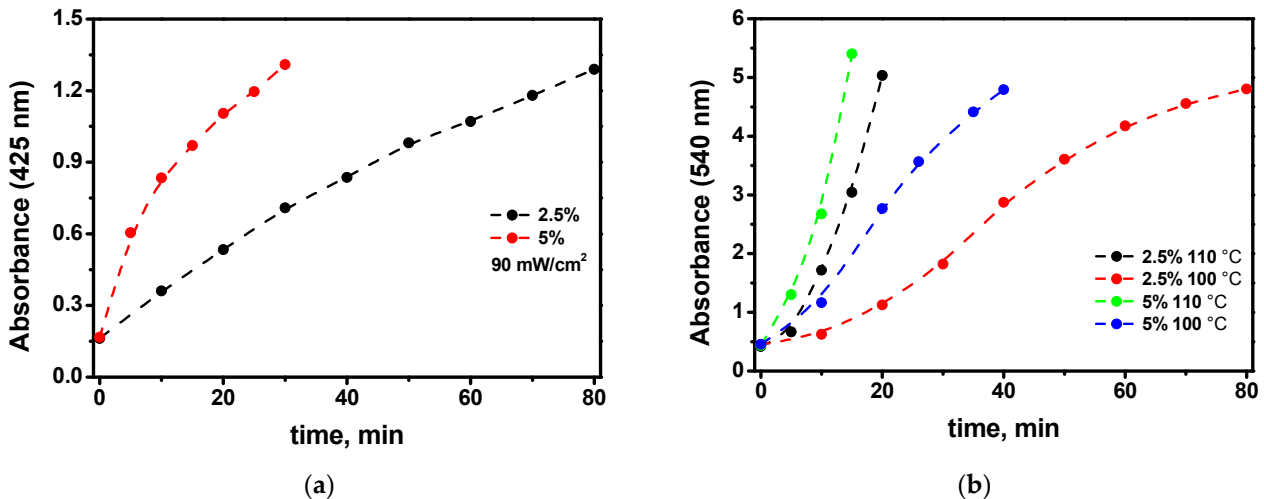


Figure 8. (a) The kinetics of absorbance growth at a wavelength of 425 nm for 2.5% and 5% films upon irradiation with a 365 nm UV LED. (b) The kinetics of the increase in absorbance at a wavelength of 540 nm upon heating at 100 and 110 °C after irradiation of 5% of the film for 30 min, and 2.5% of the film for 80 min at 90 mW/cm<sup>2</sup> (so that the absorption of the films after irradiation is the same).

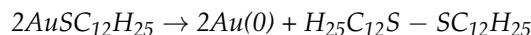
One can see (Figure 8a) that the growth of gold particles in 2.5% films occurs more slowly, both at 100 °C and at 110 °C, although the UV-induced absorption before heating was the same. Therefore, the process of the growth of nanoparticles in the samples depends on the concentration of the precursor, not only on the number of products formed due to the UV irradiation.

The data on the gold nanoparticle growth in the films at elevated temperatures below 110 °C after previous UV irradiation and the absence of this process when heating the initial films could be interpreted in such a way that the irradiation provides some ‘new’ precursor with the lower activation energy of the decomposition. In this case, the results of the heating should depend only on the magnitude of the UV-induced absorption regardless of the precursor concentration. That is, the kinetic curves for different precursor contents in Figure 8b corresponding to the same temperature should coincide. However, this is not the case.

In the works of Antolini F. et al. [6], Rogach A.L. et al. [21], and in our previous papers [24,25], the models of light-induced nanoparticle growth within polymer matrices are considered based on the reaction of obtaining the gold atom from the precursor molecule (1).

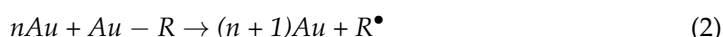


For instance, in [21], the reaction (1) looks like



The process (1) initiated by either photon absorption or elevated temperature or both provides an oversaturated solid solution of gold atoms within the matrix, causing the precipitation-phase transition where the gold nanoparticles serve as the nuclei of the new phase.

In order to qualitatively understand the experimental data on the kinetics of the gold nanoparticle growth together with the above reaction (1), we suggest considering the gold nanoparticle growth process in an alternative self-catalytic way (2)



Within this consideration, the initial centers for particle growth are provided by UV irradiation by means of reaction (1). Moreover, at elevated temperatures, the precursor molecules diffuse to these centers to implement the particle growth by reaction (2) (See Figure 9).

If this process is diffusion-limited, the rate of the accumulation of the gold atoms increases with an increase in the particle size. The saturation in the rate may be connected with the fact that residue R can adhere to the nanoparticle’s surface. The adhered residues prevent the growth process, resulting in rate saturation. This effect is evidently more pronounced at lower temperatures.

Because the rate of reaction (2) is proportional to the precursor concentration, the growth of the gold nanoparticles during the heating should be higher in the sample with a more significant precursor concentration, as seen in Figure 8.

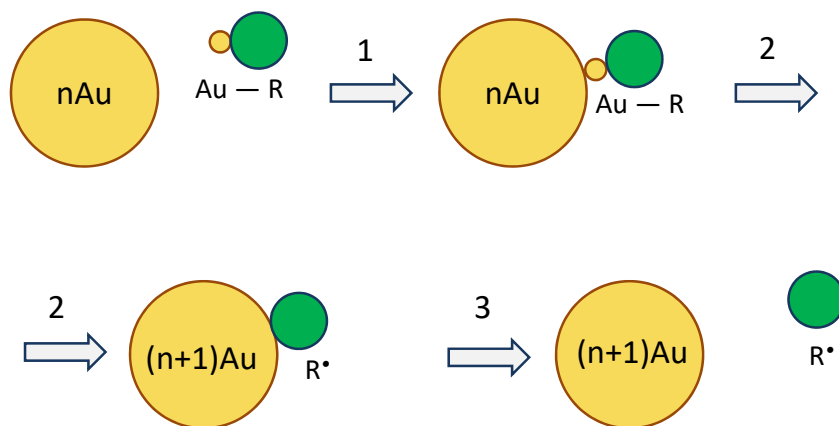


**Figure 9.** Auto-catalytic mechanism of the nanoparticle growth. The Au(I) precursor compound diffuses to the gold nanoparticle, and the reduction of gold from Au(I) occurs directly at the surface, of the nanoparticle. The residue remains for some time at the surface, preventing the attachment of the next precursor molecule.

In several works [26–28], the authors describe the autocatalytic mechanism for the reduction of gold from its Au(III) and Au(I) salts (as an intermediate) during sorption on the surface of initially formed Au(0) nanoparticles. Streszewski B. et al. [26] report on the reduction of  $[AuCl_4]^-$  salt by means of hydrazine sulfate in water solution. The authors propose the intermediate reduction of gold(III) compound to gold(I) derivative. Based on the data of kinetic studies, the authors suggest an autocatalytic character of the gold nanoparticles formation and indicate that the formation of gold nanoparticles can catalyze the reduction of Au(I) complex ions and lead to their instantaneous adsorption on the growing surface of the nanoparticles. The photoreduction of  $[AuCl_4]^-$  in a poly(*N*-vinyl-2-pyrrolidone) water-ethanol solution was studied by Harada M. et al. [27]. The authors also discuss the reduction

of gold(III) compound to gold(I) derivative, and then it is reduced by a photoinitiated radical  $\text{CH}_3\text{CH}^\bullet\text{OH}$  to gold(0) in solution or on the surface of nanoparticles. In ref. [28], the formation of gold nanoparticles was studied during the reduction of  $[\text{AuCl}_4]^-$  with L-ascorbic acid. The authors consider this reduction as the sum of three stages: (i) the reduction of Au(III) to Au(I); (ii) the process of formation of nanoparticle cores, in which Au(I) is reduced to Au(0); and (iii) the autocatalytic growth of Au(I) nanoparticles.

The autocatalytic growth of the gold nanoparticles in solution through Au(I) reduction to Au(0) directly at the nanoparticle's surface has been reported previously; however, such a mechanism for gold nanoparticle growth in a solid polymer matrix is proposed for the first time in the present work. It should be noted that, as follows from above, the Au(I) frequently serves as an intermediate compound in the reduction of Au(III). In our case, we have the Au(I) precursor from the beginning. This means that the use of such a precursor offers new opportunities for gold nanoparticle growth in polymer matrices.

#### 4. Conclusions

1. We demonstrate good-quality polystyrene films with up to 5 wt% of  $(\text{Ph}_3\text{P})\text{Au}(n\text{-Bu})$  obtained by casting technique from the solution in toluene. The films are transparent in the optical region and show no signs of scattering.
2. The UV irradiation of the films at room temperature provides the formation of an extinction band in the optical region. Subsequent heating of the UV-irradiated films results in an absorption band with a maximum near 540 nm, which is characteristic of the plasmon resonance band of gold nanoparticles in polystyrene. TEM microscopy confirms the existence of gold nanoparticles within the irradiated and heated region.
3. Without UV irradiation, the heating does not lead to any transformation of the film's optical properties during the same period of treatment. This makes it possible to obtain patterns by means of UV irradiation of the samples through a mask (see Figure 5) employing the exposure–development process when the development is the heating of the exposed film at temperatures of approximately 110 °C. These structures can be used in photonics devices because plasmon nanoparticles strongly change the optical properties of the original material, which remains intact in unexposed parts.
4. The elucidation of the kinetics of the nanoparticle growth at different precursor percentages in the films allows us to conclude that the process of the self-catalytic deposition of the gold atoms to the gold nanoparticle directly from the precursor molecule is significant (see Figure 9). This challenges existing ideas about the mechanism of the growth of gold nanoparticles in polymer films.

**Author Contributions:** Investigation, A.K., S.B., S.G., D.T., I.L., N.A., A.P. and N.B.; project administration and supervision N.B.; writing—original draft, A.K. and N.B.; and writing—review and editing, A.P. and N.B. All authors have read and agreed to the published version of the manuscript.

**Funding:** This work is supported by the Center of Excellence «Center of Photonics» funded by The Ministry of Science and Higher Education of the Russian Federation, contract № 075-15-2022-316.

**Institutional Review Board Statement:** Not applicable.

**Informed Consent Statement:** Not applicable.

**Data Availability Statement:** The data presented in this paper are available on the request from the corresponding author.

**Conflicts of Interest:** The authors declare no conflict of interest.

#### References

1. Li, H.; Liu, D.; Khan, K.; Shao, J.; Liu, X.; Cao, R.; Ma, C.; Chong, F.; Tareen, A.K.; Hu, F.; et al. Two-dimensional metal organic frameworks for photonic applications. *Opt. Mater. Express* **2022**, *12*, 1102–1121. [[CrossRef](#)]
2. Ma, N.; Horike, S. Metal–Organic Network-Forming Glasses. *Chem. Rev.* **2022**, *122*, 4163–4203.
3. Castel, N.; Coudert, F.-X. Atomistic Models of Amorphous Metal–Organic Frameworks. *J. Phys. Chem. C* **2022**, *126*, 6905–6914. [[CrossRef](#)]

4. Loste, J.; Lopez-Cuesta, J.-M.; Billon, L.; Garay, H.; Save, M. Transparent polymer nanocomposites: An overview on their synthesis and advanced properties. *Prog. Polym. Sci.* **2019**, *89*, 133–158. [[CrossRef](#)]
5. Bityurin, N.; Alexandrov, A.; Afanasiev, A.; Agareva, N.; Pikulin, A.; Sapogova, N.; Soustov, L.; Salomatina, E.; Gorshkova, E.; Tserova, N.; et al. Photoinduced nanocomposites—creation, modification, linear and nonlinear optical properties. *Appl. Phys. A* **2013**, *112*, 135–138. [[CrossRef](#)]
6. Antolini, F.; Orazi, L. Quantum dots synthesis through direct laser patterning: A review. *Front. Chem.* **2019**, *7*, 252. [[CrossRef](#)]
7. Smirnov, A.A.; Elagin, V.; Afanasiev, A.; Pikulin, A.; Bityurin, N. Luminescent patterns recorded by laser irradiation of a PMMA matrix with a soluble CdS precursor. *Opt. Mater. Express* **2020**, *10*, 2114–2125. [[CrossRef](#)]
8. Bityurin, N.; Ermolaev, N.; Smirnov, A.A.; Afanasiev, A.; Agareva, N.; Koryukina, T.; Bredikhin, V.; Kamenskiy, V.; Pikulin, A.; Sapogova, N. Plasmonic, excitonic and exciton-plasmonic photoinduced nanocomposites. *Appl. Phys. A* **2016**, *122*, 193. [[CrossRef](#)]
9. Lippman, D.H.; Kochan, N.S.; Yang, T.; Schmidt, G.R.; Bentley, J.L.; Moore, D.T. Freeform gradient-index media: A new frontier in freeform optics. *Opt. Express* **2021**, *29*, 36997–37012. [[CrossRef](#)]
10. Bityurin, N.; Kudryashov, A. Diffusion-assisted ultrashort laser pulse induced photothermal growth of core-shell nanoparticles in polymer matrix. *Opt. Express* **2021**, *29*, 37376–37398. [[CrossRef](#)]
11. Antolini, F.; Pentimalli, M.; Di Luccio, T.; Terzi, R.; Schioppa, M.; Re, M.; Mirengi, L.; Tapfer, L. Structural characterization of CdS nanoparticles grown in polystyrene matrix by thermolytic synthesis. *Mater. Lett.* **2005**, *59*, 3181–3187. [[CrossRef](#)]
12. Smirnov, A.A.; Afanasiev, A.; Ermolaev, N.; Bityurin, N. LED induced green luminescence in visually transparent PMMA films with CdS precursor. *Opt. Mater. Express* **2016**, *6*, 290–295. [[CrossRef](#)]
13. Smirnov, A.A.; Afanasiev, A.; Gusev, S.; Tatarskiy, D.; Ermolaev, N.; Bityurin, N. Exposure dependence of the UV initiated optical absorption increase in polymer films with a soluble CdS precursor and its relation to the photoinduced nanoparticle growth. *Opt. Mater. Express* **2018**, *8*, 1603–1612. [[CrossRef](#)]
14. Huang, R.; Fu, Y.; Zeng, W.; Zhang, L.; Wang, D. The facile approach to fabricate gold nanoparticles and their application on the hydration and dehydrogenation reactions. *J. Organomet. Chem.* **2017**, *851*, 46–51. [[CrossRef](#)]
15. Peña-López, M.; Ayán-Varela, M.; Sarandeses, L.A.; Pérez Sestelo, J. Palladium-catalyzed cross-coupling reactions of organogold(I) phosphanes with allylic electrophiles. *Org. Biomol. Chem.* **2012**, *10*, 1686–1694. [[CrossRef](#)]
16. Alexandrov, A.; Smirnova, L.; Yakimovich, N.; Sapogova, N.; Soustov, L.; Kirsanov, A.; Bityurin, N. UV initiated growth of gold nanoparticles in PMMA matrix. *Appl. Surf. Sci.* **2005**, *248*, 181–184. [[CrossRef](#)]
17. Carotenuto, G.; Martorana, B.; Perlo, P.B.; Nicolais, L. A universal method for the synthesis of metal and metal sulfide clusters embedded in polymer matrices. *J. Mater. Chem.* **2003**, *13*, 2927–2930. [[CrossRef](#)]
18. Carotenuto, G.; Nicolais, L.; Perlo, P. Synthesis of polymer-embedded noble metal clusters by thermolysis of mercaptides dissolved in polymers. *Polym. Eng. Sci.* **2006**, *46*, 1016–1021. [[CrossRef](#)]
19. Carotenuto, G.; Longo, A.; Repetto, P.; Perlo, P.; Ambrosio, L. New polymer additives for photoelectric sensing. *Sens. Actuators B Chem.* **2007**, *125*, 202–206. [[CrossRef](#)]
20. Longo, A.; Pepe, G.P.; Carotenuto, G.; Ruotolo, A.; De Nicola, S.; Belotelov, V.I.; Zvezdin, A.K. Optical emission studies in Au/Ag nanoparticles. *Nanotechnology* **2007**, *18*, 365701. [[CrossRef](#)]
21. Susha, A.S.; Ringler, M.; Ohlinger, A.; Paderi, M.; Li Pira, N.; Carotenuto, G.; Rogach, A.L.; Feldmann, J. Strongly Luminescent Films Fabricated by Thermolysis of Gold-Thiolate Complexes in a Polymer Matrix. *Chem. Mater.* **2008**, *20*, 6169–6175. [[CrossRef](#)]
22. Carotenuto, G.; Longo, A.; Hison, C.L. Tuned linear optical properties of gold-polymer nanocomposites. *J. Mater. Chem.* **2009**, *19*, 5744–5750. [[CrossRef](#)]
23. Pramanik, S.; Das, P. Metal-Based Nanomaterials and Their Polymer Nanocomposites. In *Nanomaterials and Polymer Nanocomposites: Raw Materials to Applications*; Karak, N., Ed.; Elsevier: Amsterdam, The Netherlands, 2018; pp. 91–121.
24. Bityurin, N.; Smirnov, A.A. Model for UV induced growth of semiconductor nanoparticles in polymer films. *Appl. Surf. Sci.* **2019**, *487*, 678–691. [[CrossRef](#)]
25. Pikulin, A.; Bityurin, N. Homogeneous Model for the Nanoparticle Growth in Polymer Matrices. *J. Phys. Chem. C* **2020**, *124*, 16136–16142. [[CrossRef](#)]
26. Streszewski, B.; Jaworski, W.; Paclawski, K.; Csapó, E.; Dékány, I.; Fitzner, K. Gold nanoparticles formation in the aqueous system of gold(III) chloride complex ions and hydrazine sulfate—Kinetic studies. *Colloids Surf. A Physicochem. Eng. Asp.* **2012**, *397*, 63–72. [[CrossRef](#)]
27. Harada, M.; Kizaki, S. Formation Mechanism of Gold Nanoparticles Synthesized by Photoreduction in Aqueous Ethanol Solutions of Polymers Using In Situ Quick Scanning X-ray Absorption Fine Structure and Small-Angle X-ray Scattering. *Cryst. Growth Des.* **2016**, *16*, 1200–1212. [[CrossRef](#)]
28. Luty-Błocho, M.; Wojnicki, M.; Fitzner, K. Gold Nanoparticles Formation via Au(III) Complex Ions Reduction with L-Ascorbic Acid. *Int. J. Chem. Kin.* **2017**, *49*, 789–797. [[CrossRef](#)]